QUANTUM PROPERTIES OF TWO-DIMENSIONAL ELECTRON GAS IN THE INVERSION LAYER OF $Hg_{1-x}Cd_xTe$ BICRYSTALS

W. Kraak, J. Kaldasch, P. Gille, Th. Schurig and R. Herrmann
Sektion Physik der Humboldt- Universität, Invalidenstr. 110
1040 Berlin, DDR

(Received 13 August 1990)

The electronic and magnetotransport properties of conduction electrons in the grain boundary interface of p-type $Hg_{1-x}Cd_xTe$ bicrystals are investigated. The results clearly demonstrate the existence of a two-dimensional degenerate n-type inversion layer in the vicinity of the grain boundary. Hydrostatic pressure up to 10^3 MPa is used to characterize the properties of the two-dimensional electron gas in the inversion layer. At atmospheric pressure three series of quantum oscillations are revealed, indicating that three electric subbands are occupied. From quantum oscillations of the magnetoresistivity ρ_{xx} the characteristic parameters of the electric subbands (subband populations n_{si}, subband energies E_F-E_i, effective electron masses m^*_{ci}) and their pressure dependences are established. A strong decrease of the carrier concentration in the inversion layer and of the corresponding subband population is observed when pressure is applied. A simple theoretical model based on the triangular-well approximation and taking into account the pressure dependence of the energy band structure of $Hg_{1-x}Cd_xTe$ is used to calculate the energy band diagram of the quantum well and the pressure dependence of the subband parameters.

1. Introduction

The electronic properties of grain boundaries in semiconductors have attracted increasing interest over the past few years.

Recently it was demonstrated by magnetotransport investigations of the electronic properties of grain boundaries in various semiconducting materials that the defects in the grain boundary region are evidently leading to the formation of a natural quantum well in which a degenerate carrier gas (inversion or accumulation layer) forms a quasi-two-dimensional system. In this system the carrier gas is confined in a symmetric V- like potential well which quantizes the motion of the carriers in the direction perpendicular to the grain boundary interface. For example, such inversion layers adjacent to grain boundaries are found in n-Ge /1,2/, p-InSb /3,4/ and p- $Hg_{1-x}Mn_xTe$ /5,6/.

Interesting properties of this disordered quasi-two-dimensional electron system have been demonstrated by the observation of characteristic quantum phenomena (subband quantization, integral quantum Hall effect, weak localisation effects). However, the nature of the interface states in the grain boundary is not yet completely clear. Dangling bonds and segregated impurities seem to be the most important defects in the vicinity of the grain boundary

0749-6036/91/040471+08 $02.00/0

interface. Detailed studies of the electrical transport properties of grain boundaries may give valuable information about the nature of defects at the interface and so are highly desirable.

Moreover, the narrow gap semiconductors (especially InSb and $Hg_{1-x}Cd_xTe$) offer an unique band structure and combination of electronic properties (extremely low effective electron masses, high carrier mobilities , high effective g-factors, nonparabolicity of the energy bands, unique composition and pressure dependence of the energy band parameters). These properties result in large Landau level spacings and pronounced quantum effects in high magnetic fields. As a consequence, these alloy systems are excellent candidates for the investigation of quantum phenomena in reduced dimensions.

In this paper we present electrical and magnetotransport properties of the grain boundary interface in p-type $Hg_{1-x}Cd_xTe$ bicrystals which indicate that a degenerate n-inversion layer exist adjacent to the grain boundaries. By means of the quantum oscillations of the magnetoresistivity, namely the Shubnikov-de Haas (SdH)- effect , the characteristic parameters of the quasi-2D electron gas and their pressure dependences were established.

2. Crystal Growth

The crystals studied were grown by the seedless travelling heater method (THM) using Te as a solvent . Starting from 5N elements combined with further purification efforts (destillation, zone melting) polycristalline source materials have been homogenized from the binary components separately synthesized before. The crystals have been grown from a Te-rich solution at a temperature of 550 °C with a growth rate of 1.0 mm per day.

A typical ingot consists of several differently oriented grains with volumes up to 1 cm^3. The polycrystalline structure can be clearly seen after selective etching in a solution of 30% HNO_3, 20% HCl and 50% H_2O (Fig.1).

$Hg_{1-x}Cd_xTe$ bicrystal samples containing a single grain boundary are cut from the as-grown ingot by a wire saw into rectangular Hall bars with maximum dimensions of 1 x 1 x 5 mm^3.

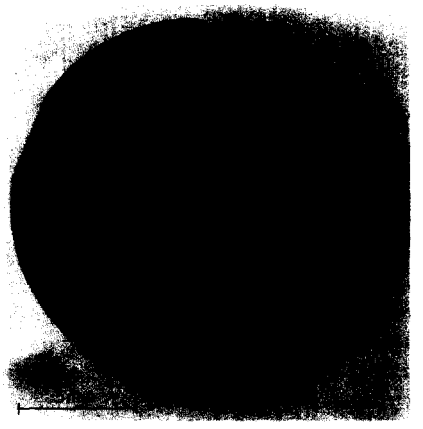

Fig. 1: Micrograph of an etched cross-section of a $Hg_{1-x}Cd_xTe$ slice showing few differently oriented monocrystalline grains. From these slices bicrystal samples containing a single grain boundary were cut.

3. Evidence for Inversion Layers in the Grain Boundary Region

Striking differences have been found for the electrical and galvanomagnetic properties of the monocrystalline and bicrystal samples:

- In contrast to the semiconducting behaviour of the bulk material the bicrystal samples revealed a metallic-like temperature dependence in the whole temperature range investigated;
- The sign of the Hall coefficient in all samples containing a grain boundary has been found negative ($R_H<0$) and to be temperature independent in the whole temperature range;
- Pronounced quantum oscillations of the magnetoresistivity ρ_{xx} have been observed in the bicrystal samples due to the quasi-2D-properties of the n-inversion layer in the grain boundary interface.

4. Quantum Properties of the 2DEG in the Inversion Layer

For various $Hg_{1-x}Cd_xTe$ bicrystal samples very pronounced SdH oscillations were observed corresponding to Landau quantization of the electron gas in the inversion layer.

Fig.2 shows a typical low-temperature SdH-plot of the magnetoresistivity component $\rho_{xx}(B)$ for a bicrystal sample.

As in the case of the inversion layer of InSb bicrystal samples /3,4/ these investigations show that the electron gas of the inversion layer in (Hg,Cd)Te grain boundaries is confined in a potential well with a scale length such that quantum effects are important ($d < \lambda_B$, where λ_B ... electron wave length). In particular, the confinement of carriers normal to the interface in the symmetric electrostatic potential gives rise to a set of electric subbands

$$E_i + \hbar^2 k_{\parallel}^2 / 2m^* \quad (i=0,1,2).$$

The application of a magnetic field perpendicular to the interface causes additional quantization: the system becomes fully quantized with energy levels given by

$$E_{i,n,s} = E_i + (n+1/2)\hbar\omega_c + s\, g\, \mu_B B.$$

As in InSb bicrystals the small effective electron mass and the small 2D density of states in $Hg_{1-x}Cd_xTe$ leads to the filling of several electric subbands.

The occupation of the higher electric subbands presumably depends on the total carrier density n_s of the inversion layer. This is clearly shown by the results summarized in Table 1, where the occupation of different subbands for inversion layers with different total electron concentrations is demonstrated.

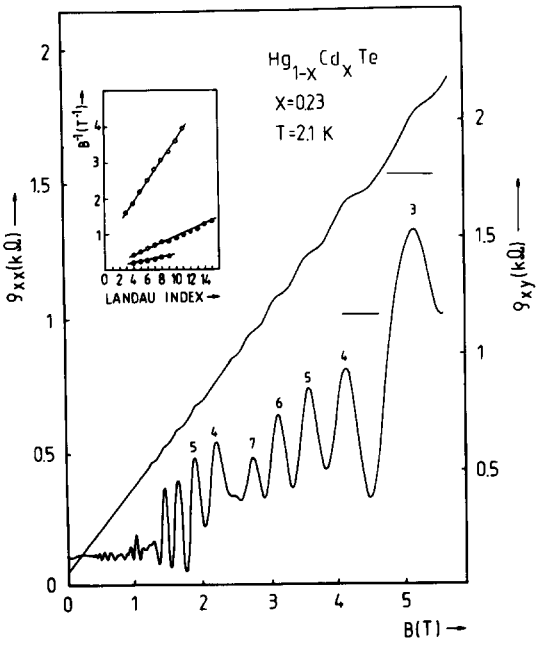

Fig. 2: Typical SdH-oscillations of the resistivity ρ_{xx} of a n-inversion layer adjacent to the grain boundary in p-$Hg_{1-x}Cd_xTe$ bicrystal (sample TH 364). The index 1 is the Landau level index of the corresponding resistivity peak. The field dependence of the Hall resistivity ρ_{xy} is also shown . The inset shows a standard SdH-plot B^{-1} vs. Landau level index for each subband.

Table 1
Subband occupation versus total inversion density n_s for different $Hg_{1-x}Cd_xTe$ bicrystals

sample	$n_s = \sum n_{si}$ (cm^{-2})	number of identified electric subbands
TH256 ($x \approx 0.2$)	1.4×10^{11}	1
TH364/12 ($x \approx 0.26$)	1.43×10^{12}	2
TH364/16 ($x \approx 0.23$)	2.0×10^{12}	3

Table 2

Experimental and theoretical parameters of the 2DEG subband structure in an $Hg_{1-x}Cd_xTe$ inversion layer (sample 364/16, $n_s = 2.0 \times 10^{12}$ cm^{-2})

parameter	experiment		theory triangular potential
	ordinary SdH plot	Fourier transform	
n_0 (cm^{-2})	$(1.07 \pm 0.01) \times 10^{12}$	1.2×10^{12}	1.17×10^{12}
n_1 (cm^{-2})	$(3.9 \pm 0.1) \times 10^{11}$	5.9×10^{11}	5.7×10^{11}
n_2 (cm^{-2})	$(1.5 \pm 0.2) \times 10^{11}$	2.35×10^{11}	2.3×10^{11}
n_3 (cm^{-2})	–	–	5×10^{10}
$n_s = \sum n_{si}$ (cm^{-2})	1.6×10^{12}	2.02×10^{12}	2.02×10^{12}
m_{c0}/m_0	0.037 ± 0.008		0.035
m_{c1}/m_0	0.023 ± 0.003		0.025
m_{c2}/m_0	0.017 ± 0.002		0.018
m_{c3}/m_0	–		0.012
$E_F - E_0$	0.105 (*) / 0.077 (**)		0.120
$E_F - E_1$	0.063 (*) / 0.061 (**)		0.073
$E_F - E_2$	0.030 (*) / 0.031 (**)		0.037
$E_F - E_3$			0.005
$n_H = 1/R_H$ (cm^{-2})	$(2.03 \pm 0.5) \times 10^{12}$		
$\mu_{4.2K}$ (cm^2/Vs)	4.0×10^4 (***)		
$\mu_{2.2K}$ (cm^2/Vs)	4.87×10^4 (***)		
$\mu_{4.2K} = \sigma R_H$ (cm^2/Vs)	4.4×10^4 (****)		

Remarks to Table 2

Material parameters used for the calculations:

x=0.23; E_g=118 meV; m_n=0.0115 m_0

$N_A - N_D = 1.0^* 10^{15}$ cm^{-3}: E_F=10 meV

The values of the cyclotron masses at the Fermi level of the corresponding subbands m^*_{ci}/m_0 have been determined from the temperatur dependence of the amplitude of SdH-oscillations. Using the values m^*_{ci}/m_0 the subband energies $E_F - E_i$ were determined in a parabolic approximation from the relation (**)

$$E_F - E_i = \frac{e\hbar}{m_{ci}\,\Delta_i(1/B)} = \frac{\hbar^2\, n_{si}\,\pi}{m^*_{ci}}$$

The subband parameters of the 2DEG in the inversion layer of sample TH 364 obtained from an analysis of the quantum oscillations and the results of self-consistent calculations using a simple triangular potential are summarized in Table 2. A good agreement between the experimental and theoretical values has been found.

Due to the strong nonparabolic character of the conduction band in $Hg_{1-x}Cd_xTe$ the cyclotron masses m^*_{ci} are different for different electric subbands. The effective cyclotron mass of the lowest subband is the highest ($\approx 0.0037m_0$) and deviates considerably from the bulk values for this composition ($\approx 0.015m_0$).

The higher subbands exhibit considerably smaller effective masses compared with the i=0 subband. The measured effective masses , which decrease with the subband number, are comparable with the calculated values.

All the features mentioned above (occupation of several subbands, strong energy dependence of the cyclotron masses m^*_{ci}) are characteristic features of 2D structures involving narrow gap semiconductors.

5. Quantum Hall Effect

In high magnetic fields (B>10T) very pronounced quantum oscillations of ρ_{xx} and pronounced spin splitting for

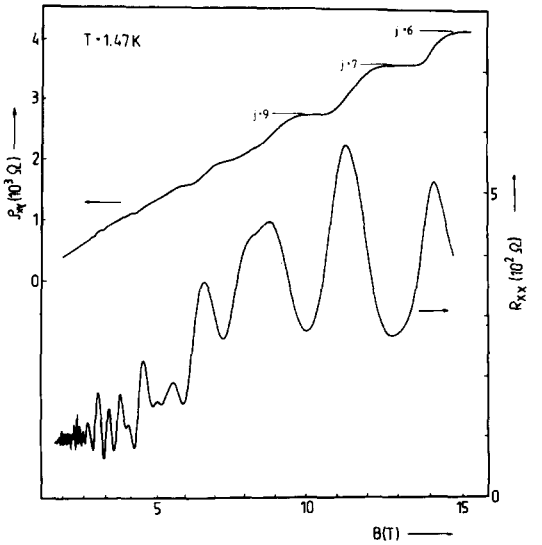

Fig. 3: Diagonal magnetoresistivity ρ_{xx} and Hall resistivity ρ_{xy} vs. magnetic field at T=1.47 K. In high magnetic fields B>10T pronounced spin splitting as well as the integral quantum Hall effect has been observed.

The values ($E_F - E_i$) (*) have been calculated with the use of Kane's nonparabolic dispersion relation:

$$E_F - E_i = -\frac{E_g}{2} \pm \left\{ \frac{E_g^2}{2} + \frac{\hbar^2 k_{Fi}^2}{2 m_n^*} E_g \right\}^{1/2} ; \quad k_{Fi} = (2\pi n_{si})^{1/2}.$$

The use of the bulk effective mass m^*_n in the grain boundary inversion layer is justified, because the interface potential spreads over many cells. It should be noted that in comparison with the values obtained from the first method the latter values (*) (nonparabolic approximation) should be more reliable.

The carrier mobilities μ have been calculated from the oscillation onset ($\mu B \approx 1$) of the subband i=2 (***) or from the electrical transport measurements using the relation $\mu = \sigma R_H$ (****).

Landau levels of the lowest electric subband (i=0) are clearly evident (Fig. 3).

Simultaneously the Hall resistivity ϱ_{xy} shows the characteristic features of the Hall plateaus. Extensive Hall plateaus with quantum numbers j=6,7 and 9 are observed; weaker plateaus are also apparent in lower fields.

A summary and comparison with the theoretical values are given in Table 3.

Table 3

$B(T)$	ϱ_{xy}^{exp} ($10^3\ \Omega$)	$j = \frac{h/e^2}{\varrho_{xy}}$	$\varrho_{xy}^{th} = \frac{h}{e^2 j}$
>15	4.19 ± 0.03	6	4.302
13.2	3.68 ± 0.03	7	3.68
10.3	2.80 ± 0.04	9	2.86

The observation of the integral quantum Hall effect in the inversion layer of (Hg,Cd)Te bicrystals demonstrate the universal two-dimensional properties of the electron gas confined in the symmetrical potential well of the grain boundary.

6. Electronic Properties of the Inversion Layer under High Hydrostatic Pressure

Hydrostatic pressure is a powerful tool to investigate the electronic properties of the two-dimensional electron gas in inversion layers.

The application of hydrostatic pressure produces significant changes in the energy bands of (Hg,Cd)Te alloys: both the direct energy gap E_g between the conduction and valence band and the effective electron mass m^* strongly increase with increasing hydrostatic compression. Thus, the electronic properties of the inversion layer in (Hg,Cd)Te grain boundaries may be affected very effectively by pressure and the investigation of the magnetotransport properties of bicrystals under hydrostatic pressure may give essentially new information concerning the parameters describing the energy band diagram of this structure.

For measuring the electrical properties under hydrostatic pressure bicrystal samples were mounted in a high pressure cell suitable for low temperature applications in high magnetic fields. High pressure (up to 10^3 MPa) was generated at room temperature and subsequently the pressure cell was placed inside the cryostat and slowly cooled down to 4.2 K.

Under hydrostatic pressure a strong variation of the electronic properties of the inversion layer is established.

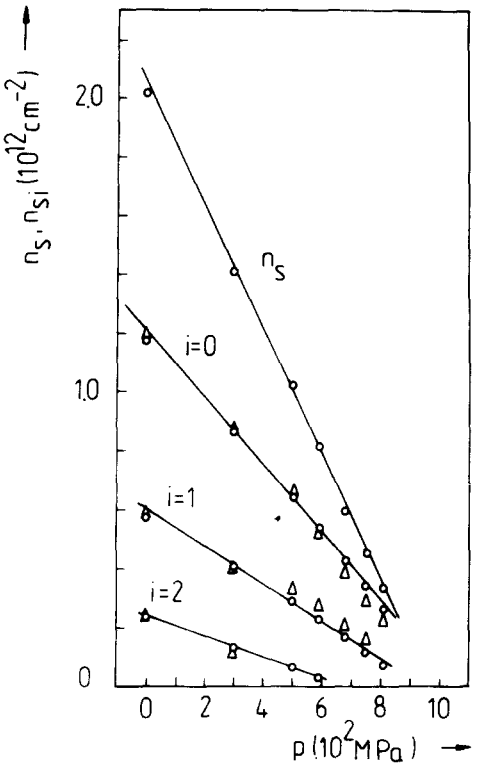

Fig. 4: Pressure dependence of the total carrier concentration n_s and the subband population n_{si} of the three electric subbands of the inversion layer (o - calculated values, Δ - experimental values).

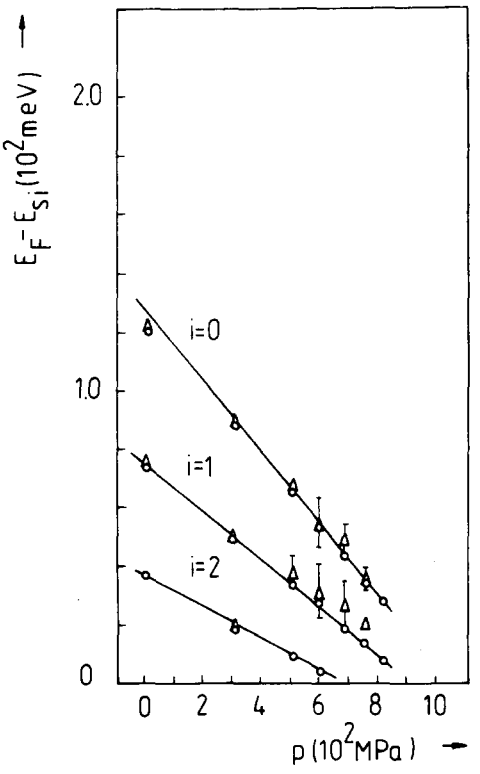

Fig. 5: Pressure dependence of the subband energies $E_F - E_i$ of the inversion layer.

A rapid decrease of the total carrier concentration n_s and the subband population n_{si} of the three electric subbands of the inversion layer is observed when pressure is applied.No inversion layer could be detected at high pressures $p>8*10^2$ MPa.

From quantum oscillations of the magnetoresistivity the characteristic parameters of the electric subbands (subband population n_{si}, subband energies $E_F - E_i$, effective electron masses m^*_{ci}) and their pressure dependences are established (Figs. 4 to 5).

A simple theoretical model based on the triangular-well approximation and taking into account the pressure dependence of the energy band gap structure of semiconducting (Hg,Cd)Te is used to calculate the energy band diagram of the quantum well and the pressure dependence of the subband parameters. The data obtained from the magnetotransport measurements are in excellent agreement with the calculated results.

7. Conclusions

1. The present results show clearly that a degenerate n- inversion layer exists adjacent to the grain boundary in p-type $Hg_{1-x}Cd_xTe$ bicrystals.

2. The rich spectrum of magnetotransport properties (SdH-oscillations, subband quantization, integral quantum Hall effect, etc.) convincingly demonstrate the quasi-2D-character of the electron gas confined in the symmetrical quantum well of the grain boundary interface.

3. The properties are typical of 2D structures involving narrow gap semiconductors with nonparabolic energy bands.

A simple theoretical calculation based on the triangular potential well approximation taking into account the nonparabolicity of the dispersion relation is in good agreement with the experimental results.

4. The results show that in suitable circumstances the inversion layer of grain boundaries in narrow gap semiconductors can be drastically alter and dominate the electrical properties at low temperatures and in high magnetic fields.

5. We have found from our magnetotransport measurements a remarkable change of the electronic properties of the n-inversion layer under high hydrostatic pressure.

A rapid decrease of the carrier concentration in the inversion layer is observed when pressure is applied.

6. The present results represent an interesting contribution both to the physics of 2D systems and the electronic structure of grain boundaries in the narrow gap semiconductor $Hg_{1-x}Cd_xTe$.

Acknowledgments - The high field experiments have been performed at the International Laboratory for High Magnetic Fields and Low Temperatures in Wroclaw (Poland).

The authors would like to thank the coworkers of this laboratory for their most valuable technical help and support in the experiments.

References

/1/ B.M.Vul and E.J.Zavaritskaya, Zh. eksper. teor. Fiz. 76, 1089 (1979).

/2/ S.Uchida, G.Landwehr and E.Bangert, Solid State Comm. 45, 869 (1983)

/3/ R.Herrmann, W.Kraak, G.Nachtwei and Th.Schurig, phys. stat. sol. (b) 129, 415 (1985)

/4/ R.Herrmann, W.Kraak, G.Nachtwei and G.Worm, Solid State Comm. 52, 843 (1984)

/5/ G.Grabecki, T.Dietl, T.Skoskiewicz and M.Gliński, Proc. Internat. Conf. Application of High Magnetic Fields in Semiconductor Physics, Würzburg 1986.

/6/ G.Grabecki, T.Dietl, P.Sobkowicz, J.Kossut and W.Zawadzki, Appl. Phys. Lett. 45, 1214 (1984).